1  REPORT

# On the origin of F-wave: involvement of central synaptic mechanisms

4  M. Görkem Özyurt,[1,2] Filipe Nascimento,[1,2] Robert M. Brownstone[2] and Marco Beato[1]

## Abstract

6  Neurophysiological methods are used widely to gain information about motor neuron excitability
7  and axon conduction in neurodegenerative diseases. The F-wave is a common biomarker used to
8  test motor neuron properties in the diagnosis of neurological diseases. Although the origin of the
9  F-wave is a subject of debate, the most widely accepted mechanism posits that the F-wave is
10  generated by the backfiring of motor neurons stimulated antidromically from the periphery.

11  In this study, we developed an *ex vivo* mouse sciatic nerve-attached spinal cord preparation with
12  sensory axons severed.

13  In this preparation, stimulation of the whole sciatic nerve or its tibial branch evoked responses
14  with the electrophysiological signatures of F-waves. Manipulations of synaptic transmission by
15  either removal of extracellular calcium or block of post-synaptic glutamate receptors abolished
16  these responses.

17  These results suggest that F-waves are mediated by spinal microcircuits activated by recurrent
18  motor axon collaterals via glutamatergic synapses.

19

20  **Author affiliations:**

21  1 Department of Neuroscience Physiology and Pharmacology (NPP), Gower Street, University
22  College London, WC1E 6BT, UK

23  2 Department of Neuromuscular Diseases, UCL Queen Square Institute of Neurology, University
24  College London, London WC1N 3BG, UK

25

1  Correspondence to: M. Görkem Özyurt

2  Department of Neuromuscular Diseases, UCL Queen Square Institute of Neurology, University

3  College London, London WC1N 3BG, UK

4  E-mail: g.ozyurt@ucl.ac.uk

5

6  Correspondence may also be addressed to: Marco Beato

7  Department of Neuroscience Physiology and Pharmacology (NPP), Gower Street, University

8  College London, WC1E 6BT, UK

9  E-mail: m.beato@ucl.ac.uk

10

13

# Introduction

15  Neurological disorders that affect motor systems, such as Amyotrophic Lateral Sclerosis (ALS)

16  and peripheral neuropathies, lead to substantial alterations in the properties of spinal motor

17  neurons. In clinical neurophysiology, electromyographic (EMG) recordings are commonly

18  employed to diagnose and understand the progression of such conditions. Electrophysiological

19  parameters such as F-wave amplitude and latency, first described by Magladery and McDougal,[1]

20  are important measurements of motor neuron and motor nerve excitability. Typically, F-waves

21  have low and variable amplitude (2-5% of the maximal direct motor response), variable latency,

22  and is subject to failures.[2] F-waves are often used to estimate motor axon conduction velocity

23  and provide valuable information about a wide range of motor disorders, such as

24  polyneuropathies and demyelinating conditions.[2,3]

25  The amplitude and latency of F-waves are both clinically useful properties. For example, a

26  sensitive marker of abnormalities in lumbosacral radiculopathies[4] is chronodispersion: the

27  difference between minimal and maximal F-wave latencies in response to a given stimulus. And

the amplitude, duration, and probability of occurrence of F-waves are used to gauge the excitability state of motor pools in a variety of central nervous system disorders.[5-8] For example, in the early stages of ALS, alterations in the excitability of motor neurons[9] correlate with increased amplitude of the F-wave.[8]

Although F-waves are routinely used for diagnosing and understanding a variety of neurological disorders, the mechanisms underlying this delayed evoked response are not fully understood. The prevalent explanation for the origin of the F-wave is that the antidromic spikes elicited by electrical stimulation of motor axons lead to somatic depolarization in a variable minority of motor neurons, which in turn leads to the generation of a second spike that is propagated orthodromically and thus recorded as a low amplitude motor response (i.e. F-wave).[2,10] While this is the generally accepted mechanism for the generation of F-waves, it is difficult to reconcile the concept of rebound spikes with the inactivation kinetics of sodium channels that would presumably prevent the generation (or propagation) of a second spike following the initial antidromic invasion. It is also notable that antidromic stimulation has been used to identify motor neurons in a variety of experimental systems *in vivo* and *in vitro*,[11,12] but the occurrence of a second "rebound" spike has never been reported.

In this report, we investigated an alternative explanation for the generation of F-waves based on anatomical studies demonstrating that motor neurons in cats are synaptically connected with other motor neurons[13,14] and functional studies showing that motor neurons in mice are synaptically connected with other motor neurons. Thus, antidromic activation of axons leads to excitation of other motor neurons (either directly or via excitatory interneurons[12,15-17]) via recurrent motor axon collaterals, a phenomenon known as recurrent excitation.[12,15] This excitation, mediated by glutamatergic transmission, can lead to orthodromic action potentials.[12] We thus hypothesized that recurrent excitation would be detected as a low-amplitude motor response in muscle recordings, and could thus underlie F-waves. Since experiments in humans are not amenable to pharmacological manipulations, we tested this hypothesis using ex vivo preparations of neonatal mouse spinal cords with sciatic nerves attached. This preparation allowed us to evoke and record the equivalent of F-waves directly from the nerves while retaining the ability to use pharmacological manipulations. We present evidence that supports the hypothesis that F-waves result from recurrent excitation of motor neurons.

## Materials and methods

All the procedures were conducted in accordance with the Animal (Scientific Procedures) Act (Home Office, UK, 1986) and were approved by the UCL Ethical Committee, under project licence number PP2688499. *Ex vivo* experiments with nerve attached were performed on tissue obtained from female (n=7) or male (n=4) mice on postnatal days 1-3 (P1-P3). Patch clamp experiments on dorsal horn ablated spinal cords were done in female (n=4) and male (n=6) wild-type mice bred on a C57Bl/6J background at P5-13. Full details of the methods are provided in the Supplementary material.

## Results

We recorded motor neurons innervating either the LG or TA muscle in dorsal horn ablated spinal cords and stimulated ventral roots in the same or adjacent segment to the recorded motor neuron (Fig. 1A). In all cases, an antidromic spike was observed following same segment stimulation (Fig. 1B - upper traces), but the subsequent EPSP was never sufficient to evoke an orthodromic spike following the antidromic one. On the contrary, stimulation of the adjacent segment invariably resulted in an EPSP that could exceed threshold and give rise to an orthodromic spike (Fig. 1B - lower traces).

We next tested whether we could prevent antidromic invasion of the soma by hyperpolarizing the motor neuron, and if in so doing, an orthodromic spike could occur. Indeed, in 14 out of 25 recorded motor neurons with antidromic spikes, hyperpolarization (between -60 and -75 mV) by direct current injection prevented somatodendritic (SD) antidromic spike but not the axon initial segment (IS) spike (Fig. 1C, left), visible as a peak in the first derivative of the voltage trace (bottom row of Fig. 1C, left). This IS spike was followed by an EPSP that did not reach threshold. Reducing the injected current (Fig. 1C, middle) enabled the EPSP to reach threshold and generate an orthodromic spike. But when the motor neuron was held at its resting membrane potential (Fig. 1C, right) the occurrence of the antidromic spike prevented the occurrence of the orthodromic one. We also compared the chronodispersion of the anti and orthodromic spikes

4

recorded and found a greater degree of chronodispersion for the orthodromic spikes than for the antidromic ones (Fig. 1D, $1.66 \pm 0.55$ ms vs. $0.39 \pm 0.29$ ms). This was not unexpected, given the EPSP reaches the threshold at different times during its rising phase.

We reasoned that in an intact system these orthodromic spikes could give rise to a delayed motor response propagating along the nerves and thus account for F-waves. We next tested if we could evoke and measure a motor response that would have the electrophysiological signatures of the F-wave (Fig. 2A). We stimulated the whole sciatic nerve (P1-3, *n=5*) and detected a large, early direct response at a more proximal sciatic site (Fig. 2B). Following this direct response, we detected a subsequent response with a latency of $29.1 \pm 5.6$ ms, with $3.9 \pm 0.8$ ms chronodispersion (CV: $0.58\pm0.08$ m/s, in the *n=3* cords in which the orientation of the nerve allowed accurate length determination). Our CV estimate is similar to the reported neonatal mice motor axon CV.[18] This second response could be regarded as an *ex vivo* analogue of the F-wave that is usually measured through EMG since it: 1) followed an initial direct motor volley, 2) did not arise from sensory axon mediated reflexes, and 3) was variable in size, shape and latency (see individual sweeps in Fig. 2B-E, chronodispersion in Fig. 2G and latency variance in Fig. 2H). Since these features matched the characteristics of the F-wave studied in clinical neurophysiology, we conclude that in our *ex vivo* neonatal mouse preparations, we were able to successfully evoke and measure F-waves from nerves.

Given our postulate that orthodromic action potentials lead to F-waves (Fig. 1) and given that we could record an F-wave equivalent (Fig. 2), we were now able to ask whether F-waves are generated by synaptic mechanisms. That is, could we abolish the F-wave response by manipulating synaptic transmission at either pre- or post-synaptic sites?

We first lowered synaptic release probability by removing $Ca^{2+}$ from the extracellular solution. Doing so did not reduce the direct response (~4% increase compared to control condition), but completely abolished the F-wave (Fig. 2C). This effect was reversible: following re-equilibration with 2 mM extracellular $Ca^{2+}$, the F-wave recovered (Fig. 2D), indicating that blocking pre-synaptic transmitter release by removing $Ca^{2+}$ is sufficient to prevent the generation of the F-wave.

Since $Ca^{2+}$ removal could also modulate motor neuron excitability, we next blocked post-synaptic receptors. Since glutamate (AMPA) receptors are known to mediate recurrent excitation

5

between motor neurons[12] and blocking them would not affect motor neuron excitability,[12] we used a selective AMPA antagonist, NBQX. We found that exogenous application of NBQX (6 µM) completely suppressed F-waves without affecting the direct motor response (~2% increase compared to control condition) (Fig. 2E). That is, we found that F-waves can be completely suppressed by either impairing the synaptic release machinery (reducing the probability of release by removing $Ca^{2+}$) or by blocking post-synaptic receptors (Fig. 2F). These results can be explained if F-waves are generated by recurrent synaptic connections, but not if they are generated by rebound spikes.

In clinical studies the F-wave is usually evoked by stimulating a single branch of the sciatic nerve. We therefore repeated our experiments stimulating only the tibial nerve and recording from the sciatic nerve using the same stimulation paradigm as above (Fig. 3A). Similar to the previous set of experiments, following tibial nerve stimulation, we detected an initial direct response, followed by a long latency event (37.1 ± 6.4 ms, CV: 0.42±0.01 m/s for *n=2*), smaller in size and with clear chronodispersion of 5.3 ± 1.3 ms (P1-3, *n=6*, Fig. 3B and F) and high latency variability (Fig. 3G). This shows that stimulation of a single branch of the sciatic nerve, in a configuration similar to that used during clinical tests, is sufficient to evoke the *ex vivo* analogue of the F-wave.

In order to confirm the synaptic identity of the F-wave recorded at the sciatic nerve following tibial nerve stimulation, we repeated the experiments blocking either pre-synaptic release or post-synaptic receptors. Blocking pre-synaptic release by removing $Ca^{2+}$ did not affect the direct response (~1% increase compared to control condition) but resulted in complete suppression of the F-wave, which was then restored upon reapplication of normal aCSF containing 2 mM of $Ca^{2+}$ (Fig. 3B and D). Similarly, blocking AMPA receptors with NBQX (6 µM) completely abolished the F-wave without affecting the initial motor response (~4% reduction compared to control condition, Fig. 3C and E). Altogether, these experiments showed that the clinically-relevant analogue, stimulation of a branch of the sciatic nerve (i.e. tibial nerve), is sufficient to generate the F-wave *ex vivo*, and that the F-wave is abolished by blocking either transmitter release or post-synaptic AMPA receptors. That is, the F-wave results from synaptic activity.

## Discussion

We used an *ex vivo* neonatal mouse spinal cord preparation with the sciatic nerve intact and showed that antidromic activation of motor axons from either the whole sciatic nerve or its posterior branch (tibial nerve), can evoke relatively long latency responses in the sciatic nerve. This response has the fundamental electrophysiological signatures of the F-wave.[2] We demonstrated that this F-wave is abolished by blocking synaptic transmission by either removing extracellular $Ca^{2+}$ or by blocking post-synaptic glutamate receptors. These observations indicate that the F-wave is synaptically generated by glutamatergic spinal microcircuits activated by synchronous motor neuron firing.

In clinical settings, low intensity stimulation of a mixed nerve generally evokes an initial H-reflex in the muscles. The gradual increase in the intensity initially results in a larger H-reflex and in activation of motor axons such that a direct motor response (M-response) is generated. However, further increment in intensity leads to an increase in the M-response while the H-reflex decreases in amplitude until it is completely abolished, due to collision of the antidromic and orthodromic motor volley.[19] After this stage, an F-wave appears, characterised by low amplitude, variable shape, and high jitter. F-waves result from activation of motor axons, possibly those innervating fast twitch muscle fibres.[20,21] Sensory afferent activation is not required, as the F-wave can still be obtained in deafferented patients or in animals with severed dorsal roots.[22] However, despite being widely used, the physiology of the F-wave is not yet understood.

The commonly accepted idea behind the F-wave is that stimulation of motor axons leads to re-excitation of the somatodendritic membrane that subsequently results in the stimulated motor neuron re-firing, giving rise to a "rebound" F-wave (Fig. 4, left side).[10,23-25] The variable shape of the F-waves across trials was attributed to different motor neurons producing the rebound firing in different trials.[26]

Here we show that, at least in *ex vivo* preparations using nerve recordings (which should be no different than EMG recording due to high safety factor of neuromuscular junctions) F-waves result from efferent-triggered central glutamate release. Antidromic invasion of motor axon collaterals can activate various circuits, including inhibitory Renshaw cell recurrent loops[27] as

well as multiple excitatory microcircuits. One of these excitatory loops is made by motor axon collaterals forming glutamatergic synaptic connections with other ipsilateral motor neurons.[12,13,28] Recurrent motor axon collaterals also activate a ventrolateral population of V3 interneurons, which in turn form glutamatergic synapses with motor neurons.[17] In addition, other circuits receiving motor collateral inputs such as ventral spinocerebellar tract neurons[15] and currently unidentified locomotor circuit neurons,[16] could also contribute to F-wave shape and duration variability by providing recurrent oligo-synaptic inputs to motor neurons. Of note, motor neuron to motor neuron connections are maintained beyond the neonatal stage and span beyond a single spinal segment.[12] These connections are ten times greater in magnitude in large post-synaptic motor neurons innervating fast twitch muscle fibres compared to small ones that innervate slow twitch fibres.[12,28] As such, synaptically-generated F-waves, as shown here, would be expected to be predominant in large motor neurons – a suggestion compatible with the clinical observation that F-waves are primarily generated by larger motor units.[20,21]

In our in vitro conditions (Fig. 1), as well as in all the in vivo recordings we are aware of, somatic invasion of the antidromic spike prevents the generation of an early orthodromic spike. In fact, an SD spike will prevent a second axonal spike generated by intracellular current injection unless the motor neuron is hyperpolarised to a point where there is a significant IS-SD delay.[29] If the motor neuron is relatively hyperpolarized at the time of arrival of an antidromic impulse (evoked by peripheral stimulation), the IS spike may not activate the SD membrane.[30] In this case, the recurrent EPSP could be sufficient to generate an orthodromic spike that, if sufficiently delayed beyond the absolute refractory period of the axon,[29] would then propagate towards the muscle (Fig. 4, right side). With F-waves being produced via orthodromic (synaptic) activation, they will be particularly sensitive to membrane voltage because the voltage would need to be hyperpolarised sufficiently to block the SD spike, and yet not so much that the EPSP does not reach threshold. In fact, it has been suggested that F-waves reflect the state of motor neuron inhibition,[6] a condition that could lead to SD spike failure. In awake animals, motor neuron membrane potentials fluctuate, meaning that at the given moment of stimulation, a variable pool of motor neurons will participate in the F-wave. That is, fluctuations of membrane voltage could account for both the observed variability in amplitude and the chronodispersion because the stochastic nature of these events would make it unlikely that the same motor neurons (with the same conduction velocities) would be recruited from trial to trial.

One limitation of our study is that we were restricted to studying neonatal animals. We note that recurrent excitatory connections are seen in mature preparations. Furthermore, although motor neuron excitability and membrane properties differ between neonatal, juvenile, and adult mice[31] and synaptic inputs change throughout development, we found no evidence of backfiring in our in vitro recordings towards the end of the second post-natal week (Fig. 1), at a time when motor neuron properties reached an advanced stage of maturation.[31] Similarly, backfiring has not been reported in adult motor neuron recordings, following antidromic invasion.[11]

Could understanding the physiology of F-waves provide any further insight into the pathophysiology of disease? For example, in people with ALS, the F-wave has reduced persistence but increased amplitude, latency, and chronodispersion. Each of these effects can be explained by "rebound" action potentials, as well as by orthodromic synaptic activation. But if synaptic activation is necessary for F-waves, then perhaps the recurrent excitation of slow motor neurons as well as inhibitory inputs (to hyperpolarise motor neurons) both increase (supplementing a homeostatic response[32]) as the disease progresses. That is, the F-wave may be sensitive to changes in synaptic inputs to motor neurons across the course of the disease.

In summary, our results indicate that the F-wave is synaptically-mediated by recurrent excitation through motor axon collaterals. Our findings provide further evidence that the F-wave reflects not only the excitability of motor neurons but also their synaptic connectivity patterns. Both of these parameters may be affected in neurological disorders and may thus impact F-waves.


# **Data availability**

Data used in this study are available within the article and its Supplementary material.

# Acknowledgements

# Funding

# Competing interests

RMB is a co-founder and is on the board of Sania Therapeutics, Inc and consults for Sania Rx Ltd.

# Supplementary material

Supplementary material is available at *Brain* online.

# References

1.	Magladery JW, McDougal Jr DB. Electrophysiological studies of nerve and reflex activity in normal man. I. Identification of certain reflexes in the electromyogram and the conduction velocity of peripheral nerve fibers. *Bull Johns Hopkins Hosp*. May 1950;86(5):265-90.

2.	Fisher MA. F-waves--physiology and clinical uses. *ScientificWorldJournal*. Feb 2 2007;7:144-60. doi:10.1100/tsw.2007.49

3. Kiers L, Clouston P, Zuniga G, Cros D. Quantitative studies of F responses in Guillain-Barré syndrome and chronic inflammatory demyelinating polyneuropathy. *Electroencephalogr Clin Neurophysiol*. Aug 1994;93(4):255-64. doi:10.1016/0168-5597(94)90027-2

4. Mebrahtu S, Rubin M. The utility of F wave chronodispersion in lumbosacral radiculopathy. *J Neurol*. Jul 1993;240(7):427-9. doi:10.1007/bf00867356

5. Fisher MA. F response latencies and durations in upper motor neuron syndromes. *Electromyogr Clin Neurophysiol*. Aug-Sep 1986;26(5-6):327-32.

6. Lin JZ, Floeter MK. Do F-wave measurements detect changes in motor neuron excitability? *Muscle Nerve*. Sep 2004;30(3):289-94. doi:10.1002/mus.20110

7. Fisher MA. F/M ratios in polyneuropathy and spastic hyperreflexia. *Muscle Nerve*. Mar 1988;11(3):217-22. doi:10.1002/mus.880110305

8. Argyriou AA, Polychronopoulos P, Talelli P, Chroni E. F wave study in amyotrophic lateral sclerosis: assessment of balance between upper and lower motor neuron involvement. *Clin Neurophysiol*. Jun 2006;117(6):1260-5. doi:10.1016/j.clinph.2006.03.002

9. Özyurt MG, Topkara B, İşak B, Türker KS. Amyotrophic lateral sclerosis weakens spinal recurrent inhibition and post-activation depression. *Clin Neurophysiol*. Dec 2020;131(12):2875-2886. doi:10.1016/j.clinph.2020.09.021

10. Mesrati F, Vecchierini MF. F-waves: neurophysiology and clinical value. *Neurophysiol Clin*. Dec 2004;34(5):217-43. doi:10.1016/j.neucli.2004.09.005

11. Meehan CF, Sukiasyan N, Zhang M, Nielsen JB, Hultborn H. Intrinsic properties of mouse lumbar motoneurons revealed by intracellular recording in vivo. *J Neurophysiol*. May 2010;103(5):2599-610. doi:10.1152/jn.00668.2009

12. Bhumbra GS, Beato M. Recurrent excitation between motoneurones propagates across segments and is purely glutamatergic. Mar 2018;16(3):e2003586. doi:10.1371/journal.pbio.2003586

13. Cullheim S, Kellerth JO, Conradi S. Evidence for direct synaptic interconnections between cat spinal alpha-motoneurons via the recurrent axon collaterals: a morphological study

using intracellular injection of horseradish peroxidase. *Brain Res*. Aug 19 1977;132(1):1-10. doi:10.1016/0006-8993(77)90702-8

14. Lagerbäck PA, Ronnevi LO, Cullheim S, Kellerth JO. An ultrastructural study of the synaptic contacts of alpha-motoneurone axon collaterals. I. Contacts in lamina IX and with identified alpha-motoneurone dendrites in lamina VII. *Brain Res*. Mar 2 1981;207(2):247-66. doi:10.1016/0006-8993(81)90363-2

15. Chalif JI, Martínez-Silva ML, Pagiazitis JG, Murray AJ, Mentis GZ. Control of mammalian locomotion by ventral spinocerebellar tract neurons. *Cell*. Jan 20 2022;185(2):328-344.e26. doi:10.1016/j.cell.2021.12.014

16. Bonnot A, Chub N, Pujala A, O'Donovan MJ. Excitatory actions of ventral root stimulation during network activity generated by the disinhibited neonatal mouse spinal cord. *J Neurophysiol*. Jun 2009;101(6):2995-3011. doi:10.1152/jn.90740.2008

17. Chopek JW, Nascimento F, Beato M, Brownstone RM, Zhang Y. Sub-populations of Spinal V3 Interneurons Form Focal Modules of Layered Pre-motor Microcircuits. *Cell Rep*. Oct 2 2018;25(1):146-156.e3. doi:10.1016/j.celrep.2018.08.095

18. Kong L, Hassinan CW, Gerstner F, et al. Boosting neuregulin 1 type-III expression hastens SMA motor axon maturation. *Acta Neuropathologica Communications*. 2023/03/30 2023;11(1):53. doi:10.1186/s40478-023-01551-8

19. Pierrot-Deseilligny E, Mazevet D. The monosynaptic reflex: a tool to investigate motor control in humans. Interest and limits. *Neurophysiol Clin*. Apr 2000;30(2):67-80.

20. Dengler R, Kossev A, Wohlfahrt K, Schubert M, Elek J, Wolf W. F waves and motor unit size. *Muscle Nerve*. Oct 1992;15(10):1138-42. doi:10.1002/mus.880151013

21. Guiloff RJ, Modarres-Sadeghi H. Preferential generation of recurrent responses by groups of motor neurons in man. Conventional and single unit F wave studies. *Brain*. Aug 1991;114 ( Pt 4):1771-801. doi:10.1093/brain/114.4.1771

22. Fox JE, Hitchcock ER. F wave size as a monitor of motor neuron excitability: the effect of deafferentation. *J Neurol Neurosurg Psychiatry*. Apr 1987;50(4):453-9. doi:10.1136/jnnp.50.4.453

23. Fisher MA. AAEM Minimonograph #13: H reflexes and F waves: physiology and clinical indications. *Muscle Nerve*. Nov 1992;15(11):1223-33. doi:10.1002/mus.880151102

24. Eccles JC. The central action of antidromic impulses in motor nerve fibres. *Pflugers Arch Gesamte Physiol Menschen Tiere*. 1955;260(5):385-415. doi:10.1007/bf00363548

25. Brock LG, Coombs JS, Eccles JC. Intracellular recording from antidromically activated motoneurones. *J Physiol*. Dec 29 1953;122(3):429-61. doi:10.1113/jphysiol.1953.sp005013

26. Panayiotopoulos CP, Chroni E. F-waves in clinical neurophysiology: a review, methodological issues and overall value in peripheral neuropathies. *Electroencephalography and Clinical Neurophysiology/Electromyography and Motor Control*. 1996/10/01/ 1996;101(5):365-374. doi:https://doi.org/10.1016/0924-980X(96)95635-0

27. Özyurt MG, Piotrkiewicz M, Topkara B, Weisskircher HW, Türker KS. Motor units as tools to evaluate profile of human Renshaw inhibition. *J Physiol*. Apr 2019;597(8):2185-2199. doi:10.1113/jp277129

28. Özyurt MG, Ojeda-Alonso J, Beato M, Nascimento F. In vitro longitudinal lumbar spinal cord preparations to study sensory and recurrent motor microcircuits of juvenile mice. *J Neurophysiol*. Sep 1 2022;128(3):711-726. doi:10.1152/jn.00184.2022

29. Gogan P, Gustafsson B, Jankowska E, Tyc-Dumont S. On re-excitation of feline motoneurones: its mechanism and consequences. *J Physiol*. May 1984;350:81-91. doi:10.1113/jphysiol.1984.sp015189

30. Coombs JS, Curtis DR, Eccles JC. The interpretation of spike potentials of motoneurones. *J Physiol*. Dec 3 1957;139(2):198-231. doi:10.1113/jphysiol.1957.sp005887

31. Sharples SA, Miles GB. Maturation of persistent and hyperpolarization-activated inward currents shapes the differential activation of motoneuron subtypes during postnatal development. *eLife*. Nov 16 2021;10doi:10.7554/eLife.71385

32. Brownstone RM, Lancelin C. Escape from homeostasis: spinal microcircuits and progression of amyotrophic lateral sclerosis. *J Neurophysiol*. May 1 2018;119(5):1782-1794. doi:10.1152/jn.00331.2017

# Figure legends

**Figure 1 Ortho- and antidromic action potentials generated in motor neurons following stimulation of ventral roots. (A)** Drawing of the dorsal horn ablated spinal cord preparation with L4 and L5 ventral root stimulation (upper) and representative images of labelled tibialis anterior (TA) and gastrocnemius (GS) motor neurons. (**B**) Current clamp recordings of ventral root evoked responses in one TA (left, 5 sweeps) and one GS (right, 2 sweeps) motor neuron from P5-13 mice, showing homosegmentally-evoked antidromic spikes (upper). At resting membrane potential, orthodromic spikes and occasional spike failures with visible EPSPs were recorded in response to adjacent root stimulation (lower, 14 sweeps for TA and 9 sweeps for GS). (**C**) Current clamp recordings of L5 ventral root evoked responses in unlabelled dorsolateral motor neurons (upper panels) showing subthreshold excitatory postsynaptic potential (EPSP), near threshold EPSP-evoked orthodromic spike, and antidromic spike. Lower panels show derivatives showing antidromic axon initial segment spikes even in the absence of somatic antidromic spikes. (**D**) Plot on the right shows chronodispersion of antidromic and orthodromic spikes. Each point indicates a motor neuron and the graph on the right is the effect size estimation plot. N is the number of motor neurons.

**Figure 2 F-waves recorded from neonatal mouse spinal cord – sciatic nerve *ex vivo* preparations following sciatic nerve stimulation depend on central synaptic release mechanisms. (A)** Schematic (left) and representative photograph (right) of the isolated spinal cord – sciatic nerve preparation, depicting the sites of stimulation (distal sciatic nerve) and recording (proximal sciatic nerve). (**B**) Example of averaged (blue trace, without peak alignment) and individual (black) traces obtained from a 2-day-old male mouse pup. Direct responses are amplified in the second averaged trace to visualise the long latency F-wave, indicated by arrows. Red lines show the estimated onset of F-waves. (**C**) $Ca^{2+}$-free aCSF abolished the F-wave, that (**D**) was restored upon reperfusion with a solution containing 2 mM $Ca^{+2}$. Red lines show the estimated onset of F-waves. (**E**) Perfusion with the AMPA receptor antagonist NBQX, also abolished the F-wave. (**F**) Plots show mean F-wave amplitudes in each animal (different colours) in different conditions and (**G**) chronodispersion of F-wave in control 2 mM $Ca^{2+}$ condition (mean ± standard deviation). (**H**) The latency variance of the direct responses and F-waves

14

shows high variance in F-wave latencies (note $\log_{10}$ scale). N is the number of *ex vivo* preparations (animals). The graph on the right is the effect size estimation plot.

**Figure 3 Stimulation of the tibial nerve also elicits F-waves that depend on central glutamate release.** (**A**) Drawing (left) and photograph (right) of the isolated spinal cord – sciatic/tibial nerve neonatal mouse preparation, depicting stimulation (tibial nerve) and recording (sciatic nerve) sites. (**B and D**) Representative averaged (blue trace, without peak alignment) and individual (black) traces obtained from a 2-day-old mouse pup, showing the direct motor responses (top row). These traces are increased in amplification (2nd row) to show the F-wave responses (indicated by arrows). The F-wave recorded in the presence of 2 mM extracellular $Ca^{2+}$ (left) was abolished in $Ca^{2+}$-free aCSF (middle) and recovered following reperfusion of 2 mM $Ca^{2+}$ solution (right). Red lines show the estimated onset of F-waves. (**C and E**) The AMPA receptor antagonist, NBQX (6 µM), abolished the F-wave (different preparations from B). Red lines show the estimated onset of F-waves. (**F**) F-wave chronodispersion at control $Ca^{2+}$ levels (mean ± standard deviation). (**G**) The latency variance of the direct response and F-wave shows high variance in F-wave latencies (note $\log_{10}$ scale). N is the number of *ex vivo* preparations (animals). The graph on the right is the effect size estimation plot.

**Figure 4 Possible mechanisms behind the F-wave.** Classical explanation is that the stimulation of motor axons antidromically leads to the re-activation of some of the motor neurons, which then triggers a "rebound" response (left). This response is recorded in the muscle as the F-wave. The mechanism proposed here is based on central synaptic glutamate release. The stimulation of motor axons leads to the generation of action potentials in some motor neurons through recurrent excitatory collaterals, activating either mono- or disynaptic excitatory microcircuits (V3 interneurons or other oligo-synaptic pathways), resulting in a "synaptic" F-wave. The motor neurons generating the synaptic F-wave are also stimulated but for representative purposes this is not shown on the figure.
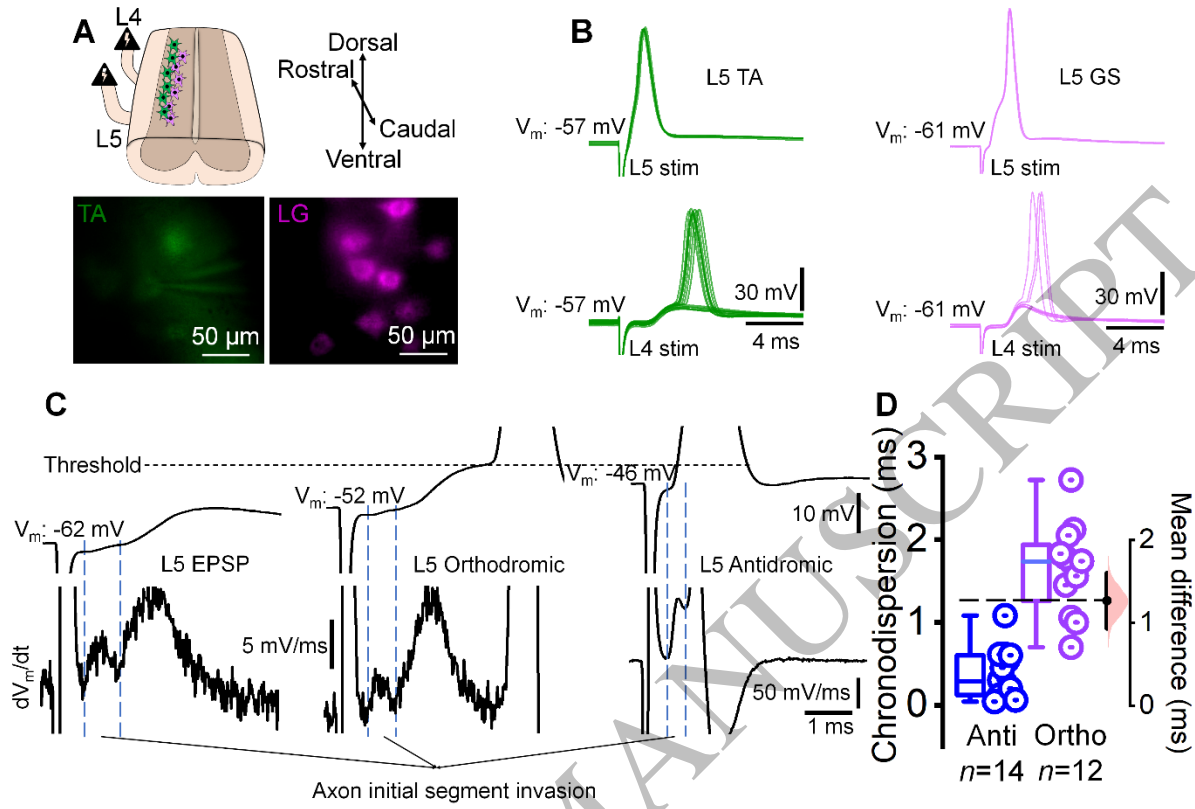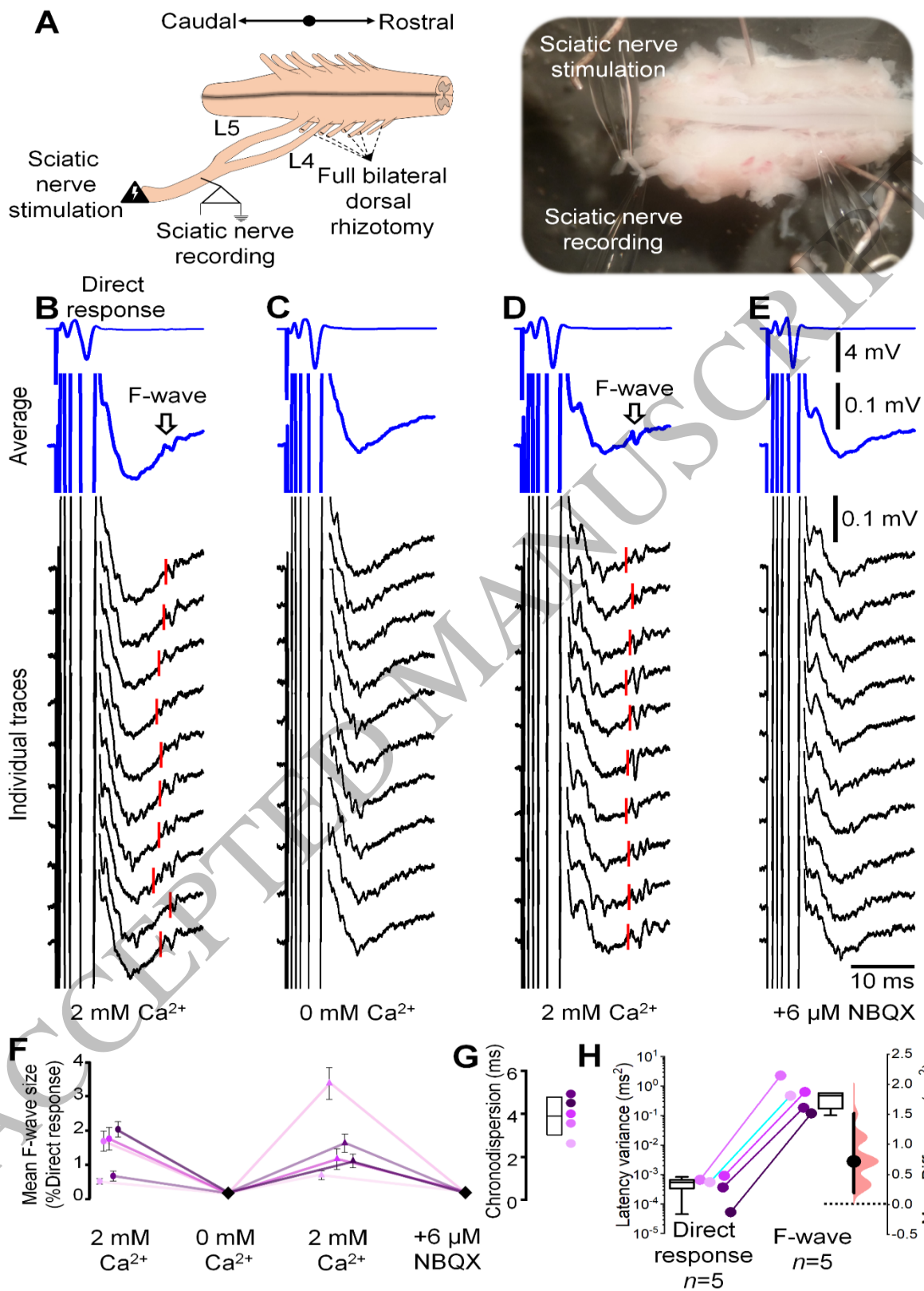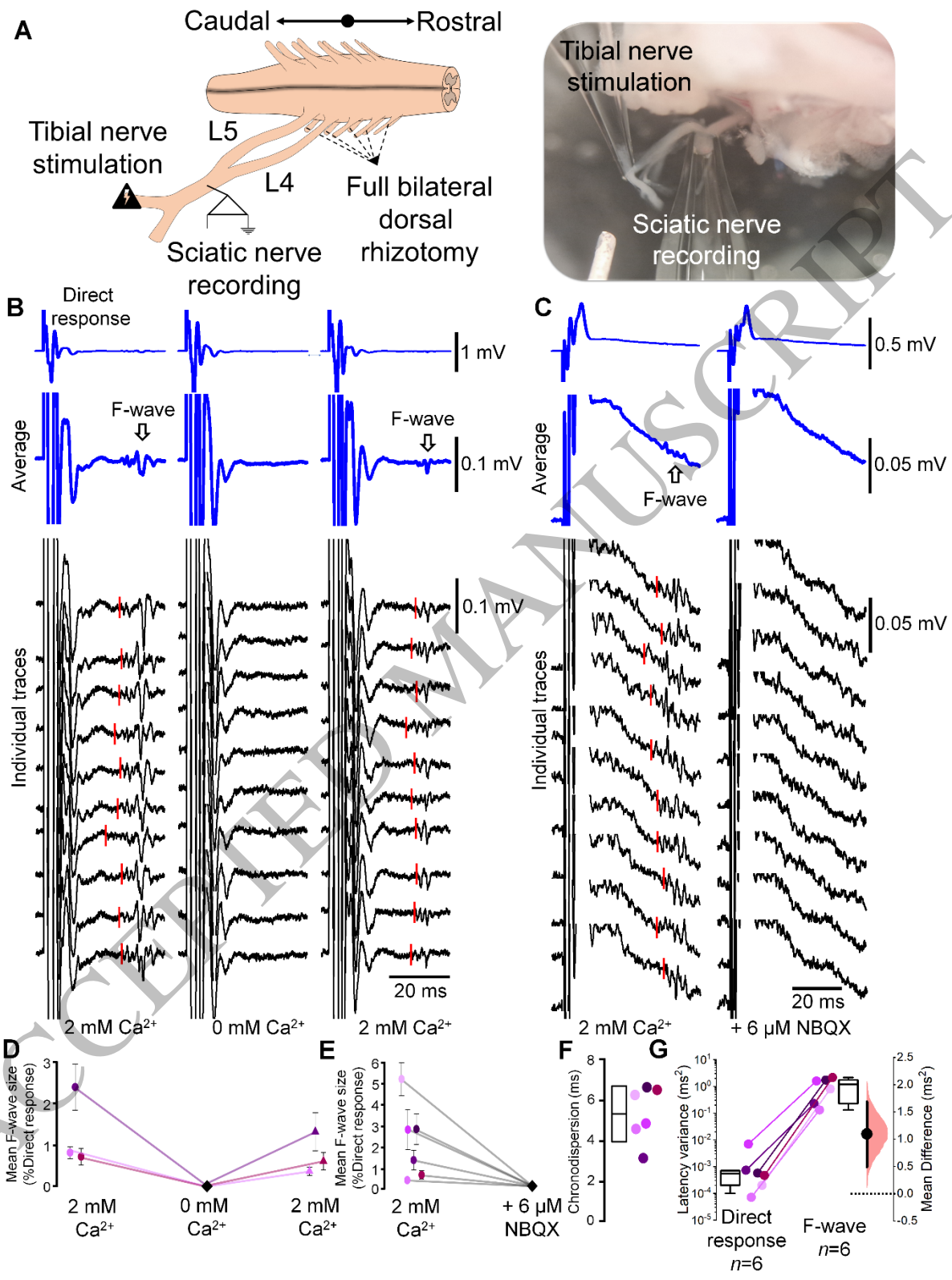
*Figure 1*
*159x107 mm ( x  DPI)*

1

2

3

4

16

*Figure 2*

*159x246 mm ( x DPI)*

1

2                                                        *Figure 3*
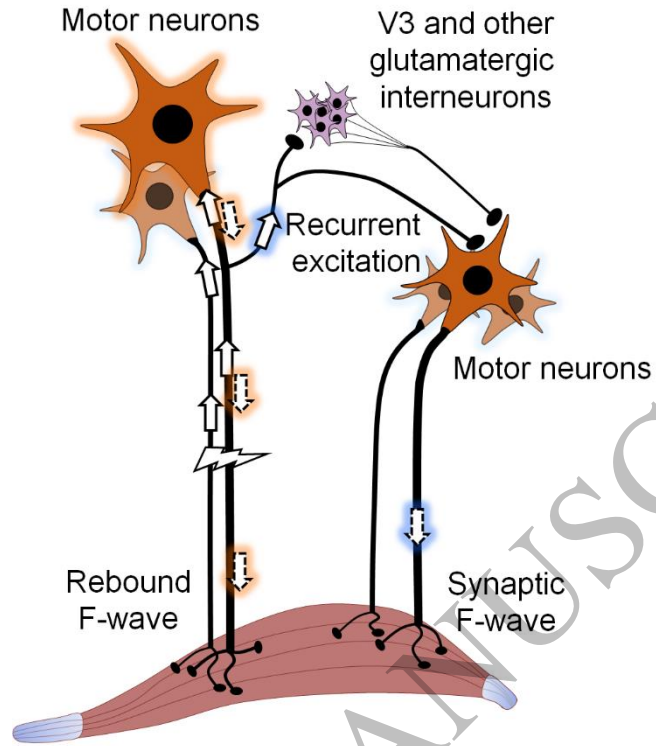3                                            *159x210 mm ( x  DPI)*

Motor neurons

V3 and other glutamatergic interneurons

Recurrent excitation

Motor neurons

Rebound F-wave

Synaptic F-wave

1
2
3

*Figure 4*
*86x101 mm ( x DPI)*